ANALYSIS

Vol.13, 2019

ISSN 2278–540X EISSN 2278–5396

DRUG DISCOVERY

Ligand efficiency: The In-Silico insight to Drug Design

Jean-Bertrand Leroux[1,2], Alexander Bukhvostov[3], Lidiya Iliyenko[3], Anton Dvornikov[3], Nimah Amirshahi[4,5], Dmitry Kuznetsov[3,6]✉

[1]Department of Biomedical Sciences, St. Joseph University, Beirut 1107, Lebanon;
[2]Department of Applied Mathematics, St. Joseph University, Philadelphia, PA 19131, USA;
[3]Department of Medical Nanobiotechnologies, Russian National Research Medical University, Moscow 117997, Russian Federation;
[4]Department of Medical Information and Computation Technologies, Amirkabir University of Technology, Tehran 159163, I.R. Iran;
[5]Department of Pharmacokinetics, University of Birmingham, Birmingham B15 2TT, UK;
[6]Department of Macromolecular Dynamics, RAS Institute for Chemical Physics, Moscow 119991, Russian Federation

✉**Corresponding author**
Department of Medical Nanobiotechnologies, Russian National Research Medical University, Moscow 117997, Russian Federation
Email: kuznano@mail.ru

Article History
Received: 14 August 2019
Accepted: 3 October 2019
Published: October 2019

Citation
Jean-Bertrand Leroux, Alexander Bukhvostov, Lidiya Iliyenko, Anton Dvornikov, Nimah Amirshahi, Dmitry Kuznetsov. Ligand efficiency: The In-Silico insight to Drug Design. *Drug Discovery*, 2019, 13, 115-128

General Note
Article is recommended to print as color version in recycled paper. *Save Trees, Save Climate*.

ABSTRACT

Ligand efficiency is a widely used design parameter in drug discovery. The dependence of ligand efficiency on the concentration unit can be eliminated by defining efficiency in terms of sensitivity of affinity to molecular size and this is illustrated with reference to fragment-to-lead optimizations. An alternative to ligand efficiency for normalization of affinity with respect to molecular size is

presented. The importance of examining relationships between affinity and molecular size directly is stressed throughout this study. To upgrade the contemporary *In Silico* drug design agenda, a novel computational version of Markov chains theory has been proposed. This is about to predict some crucial patterns of the ligand-receptor recognition and coupling.

Keywords: Markov chains, Bailey equation, *in silico* pharmacokinetics, ligand efficiency, ligand-receptor docking, drug design computational models.

1. INTRODUCTION

Most chemical starting points for design lack the affinity required to function as drugs and optimization typically results in increased lipophilicity, molecular size and molecular complexity (De Longhi, 2016; Leder et al., 2018). This highlights excessive molecular size and lipophilicity as primary design risk factors. Risks associated with molecular complexity (Katz et al., 2011; Barthels et al., 2018) are more likely to be encountered in the screening phase of a project. Molecular complexity can also be seen inversely as the degree to which a compound is structurally prototypical (Sorwall, 2017; Chandrasekhar, 2019) (e.g., minimally substituted) and might also be defined in terms of the molecular shape (Argyle & Niemer, 2016; O'Leary, 2018) of a compound or the roughness (Thallerstrom, 2017; Minz et al., 2019) of its molecular surface. Molecular recognition (Roetsch et al., 2014; Burck, 2018) provides much of the conceptual framework for drug design and many medicinal chemists consider molecular interactions (Dershey et al., 2016; Pitot, 2017) when elaborating chemical start points. While a structure-activity relationship can point to the importance of individual interactions, the contribution of a protein-ligand contact to affinity is not, in general, an experimental observable (Helinek et al., 2017; Drumm, 2018).

It would be safe to say, however, that a weak link in a row of the drug design leading events is a hard way to make a choice of the most efficient pharmacophore revealed within a paradigm of the «drug-target», i.e. «ligand-receptor», affinity docking. To optimize a solution of this dilemma, an arsenal of mathematical methods might be employed once they're focused on a modeling and testing of the above mentioned phenomena.

As per these methods themselves, they are still far of being perfect and yet there is «enough room ahead» to move forward with an attempt to upgrade the current probabilistic computational outlook for better *In Silico* ligand-receptor fitting. This attempt our present study is all about.

2. COMPUTATIONAL MODEL

Bailey Differential Equation New insight

Markov chains provide an appropriate mathematical framework for the treatment of a vast variety of theoretical and applied problems. Notably, neither exhaustive calculations of distribution parameters nor explicit expressions for probability functions are necessary in many of the applications for which knowledge of the initial momenta of the distributions proves to be sufficient. Bailey (1964, 1970, 1982) suggested a highly practical technique to this end which, however, remained largely overlooked by both theorists and practitioners as the Authors did not back it with adequate validation. Legible proof of Bailey's formula is presented in this work in a form suited for immediate practical use.

Below t stands for time and $x(t), t \geq 0$ denotes a homogeneous Markov chain with continuous time and the state space N_0 consisting of non-negative integers (the population, in the basics example considered). The process values $x(t)$ at time t are denoted as$\{x(t)\}$, and $\Delta x(t) = x(t + \Delta t) - x(t)$ is the Markov process increment (the population change over the period of time from t to $t + \Delta t$). The probability distribution at time t is determined by the probabilities $p_{x(t)}$ of the population numbering $x(t)$ species at time t.

The probability-generating function of the distribution for the process $x(t)$ is given by

$$P(z,t) = E\{z^{x(t)}\} = \sum_{x(t)\geq 0} p_{x(t)}\, z^{x(t)}$$

with $|z| \leq 1$. The transition function for the Markov process is defined by the probability distribution for $\Delta x(t)$. For a homogeneous Markov chain (provided that the transitions occur), we have, up to infinitesimal corrections $\bar{o}(\Delta t)$,

$$P\{\triangle\, x(t) = j \mid x(t)\} = f_j(x(t))\, \triangle\, t, j \neq 0, \qquad (1)$$

where the transition intensities $f_j(x(t))$ are non-negative functions depending solely on $x(t)$ for fixed values of j. It should be noted that, since the set of states $x(t)$ for the process considered is comprised of non-negative numbers, the reasonable assumption is that $f_j(x(t)) \equiv 0$ for $j < -x(t)$.

In this case, the probability that no transition occurs between t and $t + \triangle t$ is, up to an infinitesimal term $\bar{o}(\triangle t)$, given by

$$P\{\triangle x(t) = 0 \mid x(t)\} = 1 - \sum_{j\neq 0} f_j(x(t)) \triangle t. \quad (2)$$

Let $E_t(g(x(t)))$ stand for the expected value of $g(x(t))$ at time t, $g(u)$ with $u \geq 0$ being a measurable function; let $E_{t+\triangle t}(g(x(t+\triangle t)))$ be the expected value of $g(x(t))$ at $t + \triangle t$; and let $E_{t/\triangle t}\{g(x(t+\triangle t)|x(t)\}$ be the conditional expectation for $g(x(t+\triangle t))$. Also, assume that $M(\theta, t) = E_t\{e^{\theta x(t)}\} = P(e^{\theta}, t)$ with $\theta < 0$ is the Laplace-Stieljes transform of the probability distribution for process $x(t)$, which is designated as the moment-generating function; $K(\theta, t) = \ln M(\theta, t)$ is the cumulant-generating function. The cumulant-generating function is customarily represented in the form of Taylor series in θ

$$K(\theta, t) = \frac{k_1(t)}{1!}\theta + \frac{k_2(t)}{2!}\theta^2 + \cdots$$

Here k_i is the i-th cumulant of the $x(t)$ process at time $t \geq 0$. The first cumulant is equal to the expected value, the second – to dispersion, and the first cross-cumulant – to covariance (Candall & Stewart, 1966; Stewart, 1980; Dupret et al., 1997; Gorowitz, 2001).

Theorem 1

Suppose the above homogeneous Markov chain $x(t), t \geq 0$ with continuous time and with the state space N_0 is defined and its generating function $M(\theta, t)$ is differentiable. Then the generating function of the homogeneous Markov process is governed by the equation

$$\frac{\partial M(\theta,t)}{\partial t} = E_t\left[\sum_{j\neq 0}\left(e^{j\theta} - 1\right) f_j(x(t)) e^{\theta x(t)}\right], \theta < 0. \quad (3)$$

Proof. 1. Assuming that all of the expected values implied below exist, the expected value obeys the relation

$$E_{t+\triangle t}[g\{x(t+\triangle t)\}] = E_t\{E_{t/\triangle t}[g\{x(t+\triangle t)\}]\} = E_t\{E_{t/\triangle t}[g\{x(t)+\triangle x(t)\}]\}. \quad (4)$$

Given the above and as long as the expected values exist and the process is of the Markov type, the moment-generating function for the process $x(t), t \geq 0$ at time $t + \Delta t$ can be written with the help of Eq. (4) as

$$M(\theta, t+\triangle t) = E_{t+\triangle t}\left[e^{\theta x(t+\triangle t)}\right] = E_t\left[E_{t/\triangle t}\left[e^{\theta(\triangle x(t)+x(t))}\right]\right] = E_t\left[\sum_j e^{\theta[x(t)+j]}\left(f_j(x(t)) + o(\triangle t)\right)\right]$$
$$= E_t\left[e^{\theta x(t)}\sum_j e^{\theta j}\left(f_j(x(t)) + o(\triangle t)\right)\right] = E_t\left[e^{\theta x(t)} E_{t/\triangle t}\left[e^{\theta \triangle x(t)}\right]\right].$$

Therefore,

$$M(\theta, t+\triangle t) = E_t\left[e^{\theta x(t)} E_{t/\triangle t}\left[e^{\theta \triangle x(t)}\right]\right]. \quad (5)$$

2. Consider the following limit

$$\lim_{\triangle t\to 0+0} E_{t/\triangle t}\left\{\frac{e^{\theta\triangle x(t)} - 1}{\triangle t}\right\} = \lim_{\triangle t\to 0+0}\left\{\frac{P\{\triangle x(t) = 0|x(t)\}\triangle t e^{0\theta} + \sum_{j\neq 0} P\{\triangle x(t) = j|x(t)\}\triangle t e^{j\theta} - 1}{\triangle t}\right\}$$
$$= \lim_{\triangle t\to 0+0}\frac{\{(1 - \sum_{j\neq 0} f_j(x(t))\triangle t) + (\sum_{j\neq 0} f_j(x(t))\triangle t e^{j\theta})\} - 1}{\triangle t} = \sum_{j\neq 0}\left(e^{j\theta} - 1\right) f_j(x(t)).$$

Thus,

$$\lim_{\triangle t\to 0+0} E_{t/\triangle t}\left\{\frac{e^{\theta\triangle x(t)} - 1}{\triangle t}\right\} = \sum_{j\neq 0}\left(e^{j\theta} - 1\right) f_j(x(t)). \quad (6)$$

3. The derivative of the moment-generating function exists and

$$\frac{\partial M(\theta,t)}{\partial t} = \lim_{\triangle t\to 0+0} \frac{M(\theta,t+\triangle t)-M(\theta,t)}{\triangle t} = \lim_{\triangle t\to 0+0} \frac{1}{\triangle t}\left[E_t\{e^{\theta x(t)}E_{t/\triangle t}[e^{\theta x(t)}]\} - E_t[e^{\theta x(t)}]\right].$$

Since $\lim_{\triangle t\to 0+0} E_{t/\triangle t}\left\{\frac{e^{\theta \triangle x(t)}-1}{\triangle t}\right\}$ exists and depends on $f_j(x(t))$ according to Eq. (6),

$$\lim_{\triangle t\to 0+0} \frac{1}{\triangle t}\left[E_t\{e^{\theta x(t)}E_{t/\triangle t}[e^{\theta \triangle x(t)}]\} - E_t[e^{\theta x(t)}]\right] = E_t\left[e^{\theta x(t)} \lim_{\triangle t\to 0+0} E_{t/\triangle t}\left[\frac{e^{\theta \triangle x(t)}-1}{\triangle t}\right]\right] \quad (7)$$

Theorem 1 follows from Eqs. (6) and (7).

Theorem 2

If, for the above homogeneous Markov chain with $x(t), t \geq 0$, with continuous time, and with the state space N_0, the functions $f_j(x(t))$ can be presented as polynomials of the form

$$f_j(x(t)) = \sum_{k=0}^{\infty} a_{jk}\, x(t)^k, j \geq -x(t)$$

and if the derivatives implied below exist, the following differential equation holds true

$$\frac{\partial M(\theta,t)}{\partial t} = \sum_{j\neq 0}\left(e^{j\theta}-1\right)\sum_{k=0}^{\infty} a_{jk}\frac{\partial^k M(\theta,t)}{\partial \theta^k}. \quad (8)$$

Proof. Taking into account that

$$M(\theta,t) = E_t[e^{\theta x(t)}] = E_t\left[\left(e^{\theta}\right)^{x(t)}\right],$$

$$\frac{\partial M(\theta,t)}{\partial \theta} = E_t\left[x(t)\left(e^{\theta}\right)^{x(t)}\right],$$

…

$$\frac{\partial^k M(\theta,t)}{\partial \theta^k} = E_t\left[x(t)^k\left(e^{\theta}\right)^{x(t)}\right], \quad (9)$$

Eq. (1-3) can be cast in the form

$$\frac{\partial M(\theta,t)}{\partial \theta} = E_t\left[\sum_{j\neq 0}\left(e^{j\theta}-1\right) f_j(x(t))e^{\theta x(t)}\right] = E_t\left[\sum_{j\neq 0}\left(e^{j\theta}-1\right)\sum_{k=0}^{\infty} a_{jk}\, x(t)^k e^{\theta x(t)}\right] = \sum_{j\neq q0}\left(e^{j\theta}-1\right)\sum_{k=0}^{\infty} a_{jk}\frac{\partial^k M(\theta,t)}{\partial \theta^k},$$

which proves the theorem.

Theorem 3

If, for the above homogeneous Markov chain with $x(t), t \geq 0$, with continuous time, and with the state space N_0, the functions $f_j(x(t))$ can be presented as polynomials of the form

$$f_j(x(t)) = \sum_{k=0}^{\infty} a_{jk}\, x(t)^k, j \geq -x(t)$$

and if the derivatives implied below exist, the following differential equation holds true

$$\frac{\partial P(z,t)}{\partial t} = \sum_{j\neq 0}\left(z^j-1\right)\sum_{k=0}^{\infty} a_{jk}\, z^k \frac{\partial^k P(z,t)}{\partial z^k}.$$

Proof. Given that the derivatives $\frac{\partial P(z,t)}{\partial t}, \frac{\partial^k P(z,t)}{\partial z^k}$ exist and that $M(\theta,t) = P(e^\theta, t)$, the change of variables from z to e^θ yields

$$\frac{\partial P(z,t)}{\partial t} = \frac{\partial M(\theta,t)}{\partial t},$$

$$z\frac{\partial P(z,t)}{\partial z} = \frac{\partial M(\theta,t)}{\partial \theta},$$

$$z^k \frac{\partial^k P(z,t)}{\partial z^k} = \frac{\partial^k M(\theta,t)}{\partial \theta^k}. \quad (10)$$

The left-hand sides of the above expressions exist, meaning that so do the corresponding right-hand sides. Consequently, the requirements of Theorem 2 are met. Substituting Eqs. (1-10) into Eq. (8), one arrives at the result stated by Theorem 3.

The approach stemming from the above derivations is that the differential equation for the moment-generating function can be spelled out directly when the functions $f_j(x(t))$ are available. The practical applications of the above differential equations are examined below.

Outcoming Algorithms

1. Suppose that a two-dimensional homogeneous Markov chain $(x(t), y(t)), t \geq 0$ with the state space $(N_0 \times N_0)$ and continuous time is treated and that, similarly, the transition intensities are non-negative functions such that $f_{ij}(x(t), y(t)) = \sum_{k=0}\sum_{l=0} a_{ijkl}\, x(t)^k y(t)^l$. Then, if the pertinent derivatives exist, Eq. (8) affords the following generalization

$$\frac{\partial M(\theta,\varphi,t)}{\partial \theta} = \sum_{i,j}\left(e^{j\theta+i\varphi}\right)\sum_{k=0}\sum_{l=0} a_{ijkl}\frac{\partial^{k+l} M(\theta,\varphi,t)}{\partial \theta^k \partial \varphi^l}.$$

2. Consider a multidimensional Markov chain $\bar{x}(t) = \{x_1(t), x_2(t), \dots, x_n(t), \dots\}, t \geq 0$ with continuous time and the state space $\bar{N} = \{N_0 \times N_0 \times \dots N_0 \times \dots\}$, and denote $\theta = \{\theta_1, \theta_2, \dots, \theta_n, \dots\}, j = \{j_1, j_2, \dots, j_n, \dots\}$. It can be demonstrated that, provided that the pertinent expected values and derivatives exist, in the general case Eq. (3) translates into the vector equation

$$\frac{\partial M(\bar{\theta},t)}{\partial t} = E_t\left[e^{\bar{\theta}\bar{x}(t)}\sum_{j\neq 0}\left(e^{\bar{j}\bar{\theta}} - 1\right) f_j(\bar{x}(t))\right].$$

3. RESULTS

Applications of Bailey's Equation to Kinetic Schemes

First-Order Elementary Chemical Reaction

Suppose that the process of decay of substance *A* paralleled by the generation of substance *B* evolves with the probability α per molecule: $A \xrightarrow{\alpha} B$. The process is described by the function $f_{-1} = \alpha t$, and Bailey's equations become

$$\frac{\partial M}{\partial t} = \alpha\left(e^{-\theta} - 1\right)\frac{\partial M}{\partial \theta},$$

or

$$\frac{\partial K}{\partial t} = \alpha\left(e^{-\theta} - 1\right)\frac{\partial K}{\partial \theta},$$

or, alternatively

$$\frac{dk_1}{dt} = -\alpha k_1,$$

$$\frac{dk_2}{dt} = \alpha k_1 - 2\alpha k_2,$$

so that

$$k_1(t) = m(t) = a_0 e^{-\alpha t},$$

$$k_2(t) = \sigma^2(t) = a_0 e^{-\alpha t}(1 - e^{-\alpha t}).$$

Here a_0 is the initial concentration of *A*, assuming that the initial dispersion of *A* is zero.

For the simplest reversible reaction $A \underset{\beta}{\overset{\alpha}{\rightleftarrows}} B$, the formation of *B* is described by $f_1 = \alpha(a_0 - x)$ and the decomposition – by $f_{-1} = \beta x$, x being the random number of molecules of *B*. The corresponding Bailey's equation is

$$\frac{\partial M}{\partial t} = \alpha a_0\left(e^{\theta} - 1\right)M - \alpha\left(e^{\theta} - 1\right)\frac{\partial M}{\partial \theta} + \beta\left(e^{-\theta} - 1\right)\frac{\partial M}{\partial \theta}$$

or

$$k_1 = \frac{\alpha a_0}{\alpha + \beta}\left(1 - e^{-(\alpha+\beta)t}\right),$$

$$k_2 = \frac{\alpha a_0}{\alpha + \beta} e^{-(\alpha+\beta)t}\left(e^{-(\alpha+\beta)t} - 1\right) + \frac{\alpha\beta a_0}{(\alpha + \beta)^2}\left(1 + e^{-(2\alpha+2\beta)t} - 2e^{-(\alpha+\beta)t}\right).$$

Ligand-Receptor Interaction

Consider a ligand-receptor interaction $R + L \underset{\beta}{\overset{\alpha}{\rightleftarrows}} RL$, where *R* is the receptor, *L* is the ligand, *RL* is the ligand-receptor complex, α is the probability of formation of a complex molecule, and β is the probability of its dissociation. If the random number of ligand-receptor complex molecules is x, and the initial number of receptors is R_0, the number of free receptors makes $R_0 - x$. Assume that the process unfolds under the condition of large ligand surplus, so that the number of ligand molecules stays equal to its initial value L_0. The formation of ligand-receptor complexes is described by the function $f_1 = \alpha L_0(R_0 - x)$, and their decomposition – by $f_{-1} = \beta x$. Bailey's equation for the case is

$$\frac{\partial M(\theta, t)}{\partial t} = L_0 R_0 \alpha\left(e^{\theta} - 1\right)M(\theta, t) - L_0\alpha\left(e^{\theta} - 1\right)\frac{\partial M(\theta, t)}{\partial \theta} + \beta\left(e^{-\theta} - 1\right)\frac{\partial M(\theta, t)}{\partial \theta}$$

or

$$\frac{dk_1(t)}{dt} = L_0 R_0 \alpha - L_0 \alpha k_1(t) - \beta k_1(t),$$

$$\frac{dk_2(t)}{dt} = L_0 R_0 \alpha - L_0 \alpha k_1(t) - 2L_0 \alpha k_2(t) - \beta k_1(t) + 2\beta k_2(t),$$

or

$$k_1(t) = m(t) = \frac{\beta l r}{\beta l + \alpha}\left(1 - \exp\left[-(\beta l + \alpha)t\right]\right),$$

$$k_2(t) = \sigma^2(t) = \frac{\alpha\beta l r}{(\beta l + \alpha)^2}\left(1 - \exp\left[-(\beta l + \alpha)t\right]\right) + \frac{\beta^2 l^2 r}{(\beta l + \alpha)^2}\exp\left[-(\beta l + \alpha)t\right]\left(1 - \exp\left[-(\beta l + \alpha)t\right]\right)$$

Pharmacokinetic Outlook

A pharmacokinetic model of the dependence of drug concentration on time is used to gain insight into the temporal character of the emergence of dose-response relationships, the underlying assumption being that the drug is administered *per os*. In the simplest case, the process is described by the single-compartment model:

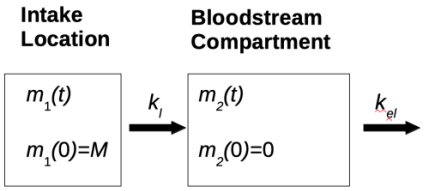

(11)

Here $m_1(t)$ is the drug mass at the intake location, $m_2(t)$ is the drug mass in bloodstream, k_l and k_{el} are the rates of drug administration and elimination from blood. The conditions that the drug is initially localized where it is being introduces are expressed as

$$m_1(t) = 0, m_2(t) = M. \tag{12}$$

The law of mass action for scheme (11) and Eq. (12) is

$$\frac{dm_1}{dt} = -k_1 m_1, m_1(0) = M,$$
$$\frac{dm_2}{dt} = k_l m_1 - k_{el} m_2, m_2(0) = 0. \tag{13}$$

The solution to the above set of equations is

$$m_1 = M \exp(-k_l t),$$
$$m_2 = M[\exp(-k_{el} t) - \exp(-k_l t).] \tag{14}$$

An analogous set of equations for a drug directly injected into the bloodstream is

$$\frac{dm_1}{dt} = 0, m_1(0) = 0,$$
$$\frac{dm_2}{dt} = -k_{el} m_2, m_2(0) = M, \tag{15}$$

its solution trivially being

$$m_1 = const = 0,$$
$$m_2 = M \exp(-k_{el} t). \tag{16}$$

The forms of the solutions to Eqs (13) and (14) are impractical, considering that the drug concentration in the bloodstream rather than its total mass is typically measured experimentally. Eqs. (13) and (14) can be conveniently transformed using the fact that drug concentration C and mass m are related as

$$C = m/V, \tag{17}$$

where V is the blood volume. The latter may actually change due to a range of factors such as, for example, the use of diuretics. However, it can be assumed if the drug does not affect diuresis that $V = const \simeq 5\,L$. Then, the combination of Eqs. (14) and (17) results in

$$C(t) = m_2(t)/V = (M/V)(\exp(-k_{el}t) - \exp(-k_l t)), \quad (18)$$

$$C(t) = C_0(\exp(-k_{el}t) - \exp(-k_l t)), \quad (19)$$

where $C(t)$ is the time-dependent drug concentration in the bloodstream and C_0 is a constant denoting its initial effective concentration. The drug concentration increases initially and subsequently decreases.

If the drug is directly injected into the bloodstream, the solution is more compact than the one defined by Eqs. (18) and (19)

$$C(t) = C_0 \exp(-k_{el}t). \quad (20)$$

The latter expression shows that in this case the drug concentration in the bloodstream decreases monotonously.

Importantly, the majority of drugs in blood bind to transport proteins rather than stay in free state. The formation of the complex involving transport protein is described by the scheme

$$H + P \overset{k}{\leftrightarrow} HP \quad (21)$$

where H is the drug, P is the blood protein, HP is their complex, and k is the dissociation constant.

The drug concentration generally tends to be much lower than that of the blood proteins. For example, the concentration of albumin, which is the key binding blood protein, is 10^{-5} M while the concentration of the nerve growth factor only reaches 10^{-9}-10^{-11} M (Alberts et al., 1994). The concentration of the growth hormone is 0.5-2.0 nM (Drawczek et al., 2018) while the concentration of the binding protein is 1.5 mM (Alonso et al., 2017). Therefore, the concentration of the drug-blood protein complexes for scheme (21) is

$$[HP] = \frac{[H_0][P]}{[H_0]+K} \quad (22)$$

(Varfolomeev & Gurevich, 1999; Brenner, 2016), where $[H_0]$ is the initial concentration of the drug. For most drugs, $K \gg [H]$ and, accordingly, Eq. (22) becomes

$$[HP] = \alpha[H_0]$$

with $\alpha = [P]/K$. Then, the drug concentration is

$$[H] = [H_0] - [HP] \approx [H_0](1-\alpha) = \beta[H_0],$$

$$[H] \approx \beta[H_0], \quad (23)$$

where β is the binding constant. The value $\beta = 1$ means that the drug undergoes no binding with blood proteins, and $\beta = 0$ shows that all drug molecules are drawn into association with blood proteins.

It may be the case that only bound drug (e.g. bilirubin) or only unbound agent (e.g. sex steroids) is excreted. In this situation, Eq. (23) is rewritten as

$$\frac{dm_1}{dt} = -k_1 m_1, m_1(0) = M,$$

$$\frac{dm_2}{dt} = k_l m_l - \gamma k_{el} m_2, m_2(0) = 0, \quad (24)$$

where γ is a constant such that $\gamma = \alpha$ if only the bound form of the drug is excreted and $\gamma = \beta$ in the opposite case. The solution to Eqs. (14-24) is

$$C(t) = C_0(\exp(-\gamma k_{el} t) - \exp(-k_l t)). \quad (25)$$

It should be noted that the underlying assumption in the analysis of biological effects which are due to the evolving drug concentration on the basis of Eq. (14-25) is that only the free form of the drug triggers response.

4. DISCUSSION

Ligand Efficiency and Molecular Dynamics

Compound-level efficiency metrics are typically constructed by either scaling (i.e., divide affinity by risk factor) or offsetting (i.e., subtract risk factor from affinity) (Waugh, 2019). LE was introduced (Dirck, 2018) as a metric to normalize affinity with respect to molecular size by scaling the standard free energy of binding, ΔG^o, by the number, N_{nH}, of non-hydrogen atoms (the term heavy atoms is also used) in the molecular structure as follows:

$$\Delta g(T, P, C^o) = \left(\frac{\Delta G^o}{N_{nH}}\right) \quad (26)$$

The standard state was not specified when the LE metric was introduced (Marshall & Bullach, 2018) although it appears to be widely believed (Marshall, et al., 2019) that C° must be set to 1 M for calculation of LE. The Achilles heel of the LE metric is its nontrivial dependency (Reuven, 2018) on C° and, as conventionally (Farrand, 2019) defined; LE has a 1 M concentration unit built into it. As noted in (Telashima & Katoh, 2017) the choice of a particular value of C°, such as 1 M, to define the standard state is entirely arbitrary and a requirement that C° only take a specific value cannot be accommodated within the framework of thermodynamics. This means that LE cannot be defined objectively in absolute terms for individual compounds because there is no physical basis for favoring a particular value of C° for calculation of LE.

Drug design guidelines are typically based on trends observed in data and the strengths of these trends indicate how rigidly guidelines should be adhered to. While excessive molecular size and lipophilicity are widely accepted as primary risk factors in drug design, it is unclear how directly predictive they are of more tangible risks such as poor oral absorption, inadequate intracellular exposure and rapid turnover by metabolic enzymes. This is an important consideration because the strength of the rationale for using LE depends on the degree to which molecular size is predictive of risk. Drug discovery scientists need to be wary of correlation inflation (Brenner & Horst, 2019) which can be loosely defined as presentation or analysis of data in any way that makes trends appear to be stronger than they actually are. Correlation inflation is a particular concern when analysis of proprietary data is presented in support of a view that a set of guidelines is especially useful or predictive.

The relevance of data must also be considered when using physicochemical characteristics such as molecular size to assess risk. For example, an activity threshold (Delbreaux et al., 2014) of > 30% inhibition at 10 μM for promiscuity analysis is not especially relevant if considering the likelihood of off-target effects for a drug with a peak unbound plasma concentration of 100 nM. Sample bias can be significant, even in large datasets, as exemplified by divergent conclusions of two apparently similar studies (Radchenko & Ludoff, 2017) with respect to the relationship between pharmacological promiscuity and molecular size. The observation that average molecular weight appears to decrease (Jelinek et al., 2017) with promiscuity is particularly relevant to the use of LE because promiscuity would generally be considered (Baglioni et al., 2018) to be an undesirable characteristic for a compound. Drug designers should not automatically assume that conclusions drawn from analysis of large, structurally-diverse data sets are necessarily relevant to the specific drug design projects on which they are working.

Thermodynamics Aspects of Ligand-Protein Association

The LE metric (Tomasetti, 2017) was introduced in thermodynamic terms and it is sometimes believed that it measures the degree to which molecular interactions between ligand and target are optimal.

The standard free energy of binding, ΔG^o, (Udvardi & Lakatos, 2017) can be written in terms of the gas constant (R), thermodynamic temperature (T), C° and the equilibrium concentrations of protein ([P]), ligand ([L]), and protein-ligand complex ([P.L]):

$$\Delta G^o = RT\, ln\left(\frac{[P][L]}{[P.L]C^o}\right) \quad (27)$$

Equation (27) shows that ΔG^o is a function of C° and this is one reason that values of standard free energy of binding should not be termed absolute. By convention, C° is taken to be 1 M although, this is arbitrary and the value of C° has no physical significance (Alonso et al., 2016). In thermodynamic analysis, a change in perception resulting from a change in a standard state definition would generally be regarded as a serious error rather than a penetrating insight. In some situations, the dissociation constant, K_D, is defined to be equal to the argument of the logarithm in equation (27) and is therefore dimensionless. However, in medicinal chemistry, biochemistry and biophysics, K_D values are conventionally quoted in units of concentration and equation (27) can be written as:

$$\Delta G^o(T,P,C^o) = RT\,ln\left(\frac{K_D(T,P)}{C^o}\right) \quad (28)$$

Equation (28) shows that a tenfold increase in C° leads to a decrease in ΔG^o of 1.36 kcal/mol at 298 K. The sign of ΔG^o has no special significance and simply indicates whether or not K_D is greater or less than C°. The dependence of ΔG^o on C° is a consequence of the stoichiometry of association of ligand with target and ΔG^o for formation of a ternary complex (relevant when considering the thermodynamic consequences of fragment linking) will exhibit a different dependence on C° to ΔG^o for a binary complex. The stoichiometry corresponding to a ΔG^o value is specified by the change, ΔN, in the number of species for the corresponding reaction and it can also be seen as a 'hidden dimension' of ΔG^o. For example, formation and dissociation of 1:1 complexes have ΔN values of –1 and +1 respectively. The value of ΔN determines the dimensions of the corresponding equilibrium constant:

$$\dim K = (concentration)^{\Delta N} \quad (29)$$

The dependence of ΔG^o on C° is a consequence of the loss of translational entropy resulting from association and it has two important implications. First, ratios of ΔG^o values also depend on C° even though the ratios themselves are dimensionless and ΔG^o values should therefore be compared as differences (i.e. ΔΔG). Second, if a free energy change is written as a sum of free energy changes then the sum needs to have the same dependency on C° as the original free energy change since the equality must hold for all values of C°. This is equivalent to requiring that the sum of ΔN values for the components of free energy decomposition be equal to the ΔN value for the free energy change that is decomposed.

One way in which stoichiometry can be accounted for in free energy decompositions is to associate each free change with its corresponding ΔN value using square brackets. The study on attribution and additivity of binding energies can be used to illustrate this: the intrinsic binding energy for a group X as the difference in ΔG^o for compounds in which X is present (AX) or absent (A) in the relevant molecular structures (Ashley, 2016):

$$\Delta G_X^i[0] = \Delta G_{AX}^o[-1] - \Delta G_A^o[-1] \quad (30)$$

The intrinsic binding energy is associated with a zero value of ΔN and is therefore independent of C°. It shows the ΔG^o value for a compound with linked groups A and B in its molecular structure as the sum of the intrinsic binding energies of A and B, and the "connection Gibbs energy" (ΔG^S):

$$\Delta G_{AB}^o[-1] = \Delta G_A^i[0] + \Delta G_B^i[0] + \Delta G^S[-1] \quad (31)$$

Equation (31) is particularly relevant to fragment linking and it is important to note that ΔG^S does depend on C° (Marciewicz, 2017). In some studies, ΔG^o is decomposed into a value corresponding to zero molecular size ($\Delta G_{MS=0}$) and a ΔΔG value (Wiespanski, et al., 2017):

$$\Delta G^o[-1] = \Delta G_{MS=0}[-1] - \Delta\Delta G[0] \quad (32)$$

One general approach to modelling affinity is to use equation (33) in which A_i (i > 0) is a parameter associated with the substructure i and ni is the number of occurrences of that substructural element:

$$\Delta G^o[-1] = A_0[-1] + \sum_{i=1}^{N_{SS}} n_i \times A_i[0] \quad (33)$$

The A0 term has the same dependency on C° as ΔG^{o} and its inclusion in equation (33) allows changes in concentration unit to be easily accounted for. The substructures are typically groups at substitution sites on a scaffold and the ni values are either 1 or 0 and A_0 may correspond to the affinity of the unsubstituted scaffold.

Schemes for decomposition of ΔG^{o} based on equation (33) cannot be considered to be group additive because of the presence of the A_0 term which is not associated with any group.

An equivalent way to examine the stoichiometry issue is to consider the implications of writing K_D as follows where k_{nH} corresponds to Δg as defined in equation (26):

$$K_D = (k_{nH})^{N_{nH}} \qquad (34)$$

Consider two compounds X (K_D = 10-3 M; N_{nH} = 10) and Y (K_D = 10-6 M; N_{nH}= 20) that would usually be considered to be equally ligand-efficient (Δg = 0.4 kcal/mol per non-hydrogen atom at 298 K for C° = 1 M). While the values of k_{nH} calculated for X (0.501 $M^{0.1}$) and Y (0.501 $M^{0.05}$) have the same numerical value, it is incorrect to equate them because their dimensions differ, as reflected by the difference in their respective units. If K_D is expressed in millimolar units, the numerical values of k_{nH} for X (1 $mM^{0.1}$) and Y (0.708 $mM^{0.05}$) are no longer identical.

Some of the entropy of binding results from molecular interactions (e.g., between water molecules) that are non-local with respect to protein-ligand contacts. Some contributions to binding enthalpy, such as the enthalpic penalties associated with ligand and target adopting their bound conformations are also inherently non-local. A less obvious example of a non-local effect would be substitution at one position of a molecular structure preventing a substituent at another position from forming optimal interactions with the target. When interpreting binding thermodynamics in terms of molecular interactions, it should always be kept in mind that intermolecular contacts (e.g., between unbound ligand and solvent) that are not present in the protein-ligand complex also influence ΔH and ΔS^{o}.

Perception of Affinity Varies with Concentration Unit

Some of the problems that result from using LE as a design metric can be seen more clearly if it is expressed using a base 10 logarithm and without energy units:

$$\eta_{bind} = -\left(\frac{1}{N_{nH}}\right) \times \log_{10}\left(\frac{K_D}{C^o}\right) = \frac{\Delta g}{RT\ln(10)} \qquad (35)$$

The quantity η_{bind} is related to Δg by a multiplicative factor of RT ln(10) that is independent of C° and therefore both quantities respond in an identical manner to a change in C°. One rationale for using η_{bind} is that drug discovery scientists typically use pIC_{50} or pK_D rather than ΔG^{o} in «drug-target» analysis. The quantity η_{bind} is also related to ligand efficiency by atomic number (LEAN) (Lepellier, et al., 2016) that is calculated by scaling pIC_{50} by N_{nH}. Unlike LEAN, η_{bind} is a function of C° and can also be written as $\eta_{bind}C^{o}$ to emphasize this. Although standard state conventions do not apply to potency measures such as IC50 and EC_{50}, which are usually quoted in μM or nM, potency must still be scaled by a concentration value for the logarithm calculation because the logarithm function is not defined for dimensioned quantities (Schramm & Kuntz, 2018). Using η_{bind} rather than ΔG^{o} reinforces the point that the problems associated with LE are due to the mathematical behavior of the logarithm function. While the use of a concentration unit other than 1 M to define LE is unusual, there certainly is precedent for doing so.

LE is used to specify affinity cutoffs as a function of molecular size and a Δg value of 0.3 kcal/mol per non-hydrogen atom has been suggested (Fouquet & Berthault, 2017). Specification of affinity cutoffs in this manner forces the line defining acceptable affinity to intersect the affinity axis at a point corresponding to a K_D value of 1 M. The minimum Δg value of 0.12 kcal/mol per non-hydrogen atom recommended (Allwerck et al., 2017) can be translated (C° = 1 M; T = 300 K) to pK_D values corresponding to the lower (700 Da; $N_{nH} \approx 50$) and upper (3000 Da; $N_{nH} \approx 214$) limits. The lower (pK_D= 4.4) of these two values would not appear to be a useful design criterion while the higher value (pK_D= 18.7) would not generally be measurable. In general, affinity thresholds should be specified directly and LE should only be used for this purpose if supported by the data.

LE features prominently in the literature of fragment-based lead discovery (Ekkert & Bauer, 2018) to the extent that it is sometimes presented as an important rationale for screening fragments.

Comparison of LE values for fragment hits and the corresponding leads can be seen as an attempt to quantify how effectively an increase in molecular size translates to affinity. This is still a valid objective even though the LE metric would appear to be unfit for this purpose. The most obvious way to do this is to scale ΔpK_D by ΔN_{nH}:

$$\frac{\Delta pK_D}{\Delta N_{nH}} = \left(\frac{1}{N_{nH}[L]-N_{nH}[F]}\right) \times \log_{10}\left(\frac{K_D[F]}{K_D[L]}\right) \quad (36)$$

Using ΔpK_D (the logarithm of a ratio of $K_D$values) eliminates the dependency on C° that makes Δn_{bind} (and Δg) unsuitable for comparison of start and end points for projects. An additional benefit is that ΔpK_D is likely to be relatively insensitive to the approximation of $K_D$by IC50. This approach to assessing optimizations has precedent (Bolton & Murdock, 2018) and reported that a tenfold improvement in K_D corresponded to a mean increase in molecular weight of 64 Da (standard deviation = 18 Da) for 73 compound pairs. Some other reports (Sieliwanowicz, 2018) also illustrate the benefit of observing the response of affinity to an increase in molecular size directly rather than indirectly by using the LE metric.

It can be useful to compare the changes in affinity and lipophilicity that result from structural elaboration and one way of achieving this is to offset the change in affinity by change in lipophilicity:

$$\Delta pK_D - \Delta \log P = \log_{10}\left(\frac{K_D[F]\times P[F]}{K_D[L]\times P[L]}\right) \quad (37)$$

The quantity in equation (37) may be regarded as a measure of the lipophilicity efficiency. It is desirable that it should be as large as possible most drug design cases studied. Variations of equation (37) can also be written using potency (e.g. pIC50) with a measured distribution coefficient (logD) or a predicted value of logP (Vagel et al., 2017).

Observation that a small structural change leads to a large change in affinity is usually informative. Group efficiency (GE) (Ochoa & Guerlasquez, 2016) is defined for the addition of a group, X, to A by scaling the value of the associated ΔΔG (ΔG^i_X as defined in (Mishito, et al., 2019)) by ΔN_{nH}:

$$GE[A \rightarrow AX] = -\left(\frac{\Delta\Delta G[A\rightarrow AX]}{\Delta N_{nH}[A\rightarrow AX]}\right) \quad (38)$$

The notation [X→Y] can be used to specify structural transformations and to indicate that a change in the value of a property such as ΔG^o, pK_D or N_{nH} has been calculated by subtracting the value of the property for compound X from that for compound Y (Jurkovic, 2017). The definition of GE expresses equation (36) in terms of free energy rather than dissociation constant and equation (37) could be used in an analogous manner to specify the efficiency of substitutions from the perspective of lipophilicity. The fundamental difference between the two metrics is that GE is independent of C° because it is defined in terms of ΔΔG. Although GE is sometimes presented as a substructural (e.g. chloro substituent) property, it is actually structural transformations (e.g. substitute hydrogen with chlorine) with which values of GE should be associated. The ΔΔG values used for calculation of GE cannot generally be interpreted as substructural contributions to affinity because summation of values of ΔΔG (ΔN = 0) cannot reproduce the dependency of ΔG^o (ΔN = – 1) on C°.

Maximal Affinity of Ligands

Drug discovery scientists typically need be able to address a range of questions when interrogating project data. For example, it may be useful to focus analysis on the most active compounds in an optimization project. It is important to stress that residuals are not generated in isolation and they result from analysis that, arguably, should be performed anyway. The line fit to a plot of affinity against molecular size is likely to be a better predictor of outcome than a line that has been artificially forced to intercept the affinity axis at a point corresponding to a K_D value of 1 M (Von Trotta & Lemke, 2019). The strength of the trend also provides an indication of how useful normalization of the data is likely to be. For example, the observation of a very weak correlation between affinity and molecular size for hits from a fragment screen suggests that molecular size need not be accounted for when assessing the fragment hits in question. In an optimization project, a relatively weak correlation between affinity and molecular size may point to the extent that it cannot be adequately explained by molecular size alone.

5. CONCLUSIONS

A neglected Baileyan computational approach is now modified to renovate and improve the *In Silico* pharmacokinetic modeling suitable for either preclinical trail planning or the drug- receptor docking scenaria analysis. This was found a promising research tool for the «drug-target» interaction analysis required by a contemporary drug design paradigm.

LE has been discussed in depth from a physicochemical perspective in this study and the difficulty of interpreting affinity in terms of molecular interactions was highlighted. The nontrivial dependency of LE on the concentration unit in which affinity is expressed

means that LE has no physical significance and, strictly, should not even be considered to be a metric. As such, LE is unsuitable for ranking compounds, setting acceptability thresholds for affinity and modeling relationships between affinity and molecular size. While it does not appear to be possible to quantify efficiency of binding objectively for compounds in an absolute manner, efficiency can still be defined in a relative manner by scaling affinity differences by the corresponding molecular size differences.

Abbreviations

C°, standard concentration, GE, group efficiency; IC_{50}, half maximal inhibitory concentration; K_D, dissociation constant; LE, ligand efficiency; logD, base 10 logarithm of octanol/water distribution coefficient; logP, base 10 logarithm of octanol/water partition coefficient; N_{nH}, number of non-hydrogen atoms in a molecular structure; P, octanol/water partition coefficient; pIC_{50}, $-\log_{10}$(IC50/M); pK_D, $-\log_{10}$(pKD/M); pK_D[expt], experimentally measured pK_D; pK_D[pred], value of pK_D predicted by model; pK_D[resd], residual pK_D; R, gas constant; T, thermodynamic temperature; TIP, target interaction potential; Δg^o, ligand efficiency calculated from standard free energy of binding ; ΔG^o, standard free energy of binding; ΔN, change in number of chemical species; η_{bind}, ligand efficiency calculated from logarithmically expressed K_D without energy units.

Acknowledgements

This work was performed as a route of the Acad. Pontifica Middle East Laurentian Program, MELP-CJ109-20. Authors are grateful to Dr. Santiago Camacho (Dept. Mathematics and Computer Science, Wesleyan University - Bloomington, IL) for stimulating comments on preliminary findings.

Funding: This study has not received any external funding.

Conflict of Interest: The authors declare that there are no conflicts of interests.

Peer-review: External peer-review was done through double-blind method.

Data and materials availability: All data associated with this study are present in the paper.

REFERENCE

1. Alberts A, Kornberg GT, Finkel G (1994) *Neuroimmunochemistry*, Adler & Adler: Sydney-Melbourne.
2. Allwerck IG, Mamouth S, Sarkar AH (2017) Thermodynamics of the affinity coordinating sites in pI-variable proteins to reveal an optimal mode for the ligand release-n-uptake. In: *Protein Physics. I.* (Samed-Zadeh M, Ed.), pp. 71-79, Amirkabir UT-Press: Tehran.
3. Alonso S, Marshall JN, Telashima T (2017) *Contradictions in Blood Biochemistry*, Duke University Publ.: Durham, NC.
4. Alonso S, Ruttenberg K, Weiss K (2016) *Thermodynamics of Drug Turnover*. University of Salamanca: Salamanca.
5. Argyle JAS, Niemer K (2016) A molecular shape in the drug-receptor coupling. In silico models. In: *Studies on Molecular Pharmacology* (Kamensky AT, Ed.), pp. 61-77, St. Andrew's Publ., Ltd.: Aberdeen.
6. Ashley T (2016) The Energy landscape analysis for a rough ligand-protein surface imaging. *Lectures on Molecular Imaging*, Leture 12, Brown University: Providence, RI.
7. Baglioni G, Tomasetti C, Quozzo A (2018) Ligand-receptor unity re-examined. *Folia UCSC-Rome*, XXIX: 201-216.
8. Bailey NTJ (1964) *The Mathematical Approach to Biology and Medicine*. John Wiley & Sons, Ltd.: London.
9. Bailey NTJ (1970) *Statistical Methods in Biology*. 6th Edition, Cambridge University Press: Cambridge-London.
10. Bailey NTJ (1982) *Stochastic Processes in Biology and Medicine*. 11th Edition, Adler & Adler: Sydney-Melbourne.
11. Barthels SS, Sheldon DJ, Jackson L, Carter D (2018) Pharmacological screening in the drug discovery scenario. *Models in Molecular Medicine*, series A, Vol. XXIV, pp. 441-458, University of Perth Publ., Ltd: Perth-Adelaide-Melbourn.
12. Bolton S & Murdock DJ (2018) Thermodynamics scaffold in the ligand size affected drug design algorithms. In: *Advances in Molecular Pharmacology* (Ochoa M & Dunningham RJ, Eds.), pp. 3-12, University of Boston: Boston, MA.
13. Brenner A & Horst HJ (2019) Correlaton inflation in the drug discovery data. *FDA Protocols A16-A27*, FDA: Washington, DC.
14. Burk HA (2018) *Pharmacophore Docking: Models in Action.*UNL: Beirut.
15. Candall L & Stewart JA (1966) *Dispersion Analysis*. Galois Publ.: Montpellier.
16. Chandrasekhar S (2019) *The pharmacophore phenotyping. Advances and methods*. Research Triangle Press, Inc.: Ralleigh, NC.
17. De Longhi MS (2016) Structural limitations in drug design outlook. In: *Perspectives in Pharmaceutical Chemistry* (Sorenssen J, Ed.), pp. 26-42, Duke University Press: Durham, NC.

18. Delbreaux JJ, Villnois D, Moulenc-Brichard A (2014) Risk assessment in bioactive compounds taxonomy. In: *Xenobiochemistry* (Dupret S & Marchand C, Eds.), pp. 216-233, Montpellier University School of Medicine: Montpellier.
19. Dershey IN, Hrvanek A, Dogherty W (2016) Molecular and supramolecular interactions in medicinal chemistry. In: *Chemistry of Drug Receptors* (Vaughan L & Skobelev I, Eds.), pp. 143-157, WCU Press: Danbury, CT.
20. Dirk LJ (2018) *Affinity Docking. Thermodynamics Beyond*. Lectures on Molecular Dynamics, Rijken: Durban-Johanesburg.
21. Drawczek JA, Dupret J, Shatsky KK (2018) *Growth Stimulating Factors in the Amino Acids Turnover*. Proceeding of 6th International Meeting on Reproductive Biochemistry, pp. 40-61, University of Ghent Press: Ghent-Antwerp.
22. Drumm NN (2018) The structure-activity relationships in multifunctional ligand complexes. In: *Pharmaceuticals Upgraded* (Larski M & Brenner LJ, Eds.), pp. 18-30, Upjohn Publ., Inc.: Brownsweek, NJ.
23. Dupret JJ, Leroy S, Sanchez A (1997) *Theory of Systems for a Forthcoming Medicine*. Polytech Press: Rennes.
24. Ekkert H & Bauer L (2018) Pharmacophore docking in protein targets. In: *Protein Physics. II.* (Samed-Zadeh M, Ed.), pp. 303-310, Amirkabir UT-Press: Tehran.
25. Farrand W (2019) Thermodynamics of the protein signaling function. In: *Biothermodynamics* (Quarrell ST & Nerchin TS, Eds.), pp. 88-100, Blackwell Publ.: Weinheim.
26. Fouquet M & Berthault M (2017) A nature of affinity in ligand-protein pairs: Molecular size matters. *St. Joseph University Seminars on Chemistry of Life,* S18 Booklette, USJ: Beirut.
27. Gorowitz B (2001) *Asymmetrical Coupling in the Game Theory*. Bar Ilan: Ramat Gan.
28. Helinek H, Thornbach WJ, Liu K (2017) Protein-ligand affinity. Quantitative analysis and the key patterns prediction. In: *Pharmaceutical Biometrics* (Ballock T, Ed.), pp. 307-319, Charles University Libra AS: Prague.
29. Jelinek H, Vrancek A, Mlody C (2017) Ligand efficiency outlook. *Proceeding of 3rd European Conference on Medicinal Chemistry*, pp. 26-34, Charles University: Prague.
30. Jurkovic M (2017) Energy landscape analysis in the drug-target conformational modeling. In: *Medicinal Supramolecular Complexes* (Miloradovc A & Dragic D Eds.), pp. 281-294, KRKA: Ljublana.
31. Katz AJ, Ioshida K, Loddy BS, Schramm K (2011) A complexity related risks in drug design research. *Proceeding of the 9th European Meeting on Drug Design*, pp. 41-62, Alba Regia Publ.: Szeged.
32. Leder S, Ashley S, Barrow JC, Rosenbrough LC (2018) Molecular complexity in the drug targeting studies. In: *Medicinal Chemistry and Biochemistry* (Bielka H & Rapoport GA, Eds.) pp. 321-336, Laurentian University Press: Sudbury, ON.
33. Marciewicz A (2017) Energy diffusion-scattering outflow in protein dynamics affected by the low molecular mass ligands. In: *Progress in Physics of Biosystems* (Wiespanski B, Ed.), pp. 66-78, Jagellon Publ.: Krakow.
34. Marshall LM & Bullach OS (2018) Ligand efficiency: a notion of controversy. In: *Supramolecular Complexation* (Donovan L, Ed.), pp. 207-218, Northwestern Publ.: Chicago-New York-Boston.
35. Marshall LM, Meier D, Levandowski B (2019) Trimmer effect in the ligand efficiency measurements. In: *Protein Signaling Function* (Beitollahi A & Munk JS, Eds.), pp. 605-619.
36. Minz K, Rattenau K, Bluementhal JA (2019) A surface landscape in the ligand docking interfaces. In: *Progress in Supramolecular Imaging* (Yagel G & Daman S., Eds.), pp. 100-122, Abraham Weizman Inst. Sci.: Rehovot.
37. Mishito H, Ishida H, Ogata J, Ashiro O (2019) The affinity site nanotopology to determine a group efficiency in protein-ligand recognition. Quantitative analysis and medicinal outlook. In: *Medical Nanochemistry* (Telashima T, Ed.), pp. 661-673, Fuji Foundation: Tokyo-Kyoto.
38. O'Leary S (2018) *Models in Pharmacophore Studies*, Trinity College Publ.: Dublin.
39. Ochoa M & Guerlasquez J (2016) Group efficiency in ligand-protein coupling. Pharmacological and biomedical perspectives. In: *Trends in Physico-Chemical Medicine* (Santero M & Valeri J, Eds.), pp. 98-108, Valdez Camajo: Mexico City.
40. Pitot H (2017) *Logistics and Logic in the Drug Discovery Paths*. McGill: UBC Press: Vancouver.
41. Radchenko IS & Ludoff (2017) Homology lines analysis in drug discovery mode of selection. In: *Medicines on Alert* (Rijk Jn & Vernault M, Eds.), pp. 340-357, Montpellier University School of Medicine: Montpellier.
42. Reuven LL (2018) Drug-receptor fitting in membrane biophysics. In: *Membranes* (Castro A, Rouney J, Brauchet M, Eds.), pp. 98-116, Bar Ilan: Ramat Gan.
43. Roetsch K, Wallenberg A, Lemke D, Ewald-Zanossky WJ (2014) Molecules to recognize. Conditions and impacts. *Proceeding of 4th International Symposium on Drug Side Effects*, pp. 223-229, FU-Berlin, GmbH: Berlin.
44. Schramm D & Kuntz A (2018) Cytotoxicity patterns to correlate with the atomic number related ligand efficiency in drug design studies. *St. Joseph University Seminars on Chemistry of Life,* S22 Booklette, USJ: Beirut.
45. Sieliwanowicz B(2018) A quantification of drug-target binding turning points. In: *Advances in Molecular Pharmacology* (Ochoa M & Dunningram RJ, Eds.), pp. 49-61, University of Boston: Boston, MA.
46. Sorwall OS (2017) Structural prototypes in the recent drug developments. *Lectures and Seminars on Pharmaceutical Science*, University of Manitoba Publ.: Winnipeg, MB.
47. Stewart M (1980) The Laplace-Stieljes probability variatives in wholistic model of simple complexes. In: *Advances in Biometrics* (Neigel K & Frost KJ, Eds.), Vol. III, pp. 1022-1044, Westinghoffer series on Quantitative Biology, Kraft & Schoeber, GmbH: Salzbourg.
48. Telashima T & Katoh S (2017) *Pharmacophores Screening*. Sumitomo Chemical Co., Ltd.: Utajima.

49. Thallerstrom J (2017) *Medical Nanotechnologies*. Arrhenius W&S: Lund.
50. Tomasetti C (2017) Ligand-receptor coupling. Thermodynamics beyond. *Folia UCSC-Rome*, XXVIII: 88-96.
51. Udvardi L & Lakatos I (2017) Low molecular compounds to affect the protein dynamics in biosystems. In: *Studies on Molecular Hierarchy in Chemistry and Biochemistry* (Devenji S & Orban L, Eds.), pp. 444-453, Alba Regia: Budapest.
52. Vagel RL, Drumm S, Pollack JA, Turro S (2017) A computational model for toxicity prediction in the protein-binding ligands screening. In: *Biomodels* (Barthels W, Ed.), pp. 216-225, CSU Publ.: Boulder, CO.
53. Von Trotta K & Lemke H (2019) *The Drug-Target Affinity: A Nanotopology Insight*. Novartis: Basel-Geneve-Bern.
54. Waugh ICW (2019) Computational novelties in the protein-ligand affinity studies. In: *Methods in Molecular Medicine* (Ueda S, Taichi K, Watanabe I, Eds.), pp. 179-191, University of Nagoya: Nagoya.
55. Wiespanski B, Wydgoscz J, Niemer C (2017) A molecular dynamics of the ligand releasing proteins. In: *Progress in Physics of Biosystems* (Wiespanski B, Ed.), pp. 3-18, Jagellon Publ.: Krakow.